Applied Ocean Research 80 (2018) 220–227

Contents lists available at ScienceDirect

Applied Ocean Research

journal homepage: www.elsevier.com/locate/apor

Experimental studies on initiation of current-induced movement of mud

Bing Yang[a], Yang Luo[a], Dongsheng Jeng[c], Jun Feng[a,*], Aode Huhe[b]

[a] School of Civil Engineering, Southwest Jiaotong University, Chengdu 610031, China
[b] The Key Laboratory of Hydraulic and Ocean, Institute of Mechanics, Chinese Academy of Sciences, Beijing 100190, China
[c] School of Engineering and Built Environment, Griffith University Gold Coast Campus, QLD 4222, Australia

ARTICLE INFO

Keywords:
Mud
Critical flow velocity of erosion
Shear stress of initiation movement of sediment
Grey value
PIV

ABSTRACT

The initiation movement of mud exposed to currents was investigated experimentally. The initial movement of mud with different sedimentary densities was determined by measuring the flow velocity and grey level of water's image synchronously. A new method to determine the initiation movement of mud is provided (i.e., the method of relative grey value of water's image in the flume). The experimental results show that the initiation movement of mud can be classified as slight erosion and chunk erosion. The sediment concentration on a muddy bed is low for the slight erosion, and the variation in water's relative grey level is of the order of ~10. The sediment concentration for the chunk erosion corresponding to a jump in the curve of relative grey value clearly increases, and the variation in relative grey value at that instant is larger than 20. The critical flow velocity, critical friction velocity, and critical shear stress of initiation of movement of mud increase with the increase in deposit density.

1. Introduction

Muddy coasts widely exist in the world, andthe sediment at the muddy coasts is mainly composed of mud. The initial movement of mud in the tidal current significantly affects the maintenance of muddy coasts. The initiation of movement of noncohesive particles has been widely studied, and this process is relatively well understood [1–5,7]. For cohesionless sediments, the main resistance to erosion is provided by the submerged weight of sediment. However, in cohesive beds, the net attractive interparticle surface forces, frictional interlocking of grain aggregates, and electrochemical forces control the resistance to erosion and detachment. These forces vary with the type of clay, prior moisture conditions, type of shear application, and drainage conditions [6,8]. According to a study [9], the cohesion of soils significantly affects the deformation. Recently, Perret et al. [10] conducted experiments on the initiation condition of gravel–silt sediment mixtures; the effects of fine sediments were evaluated by testing beds with sand, artificial fine sand, or cohesive silt infiltrated in the gravel matrix.

The main mechanisms that cause the movement of sediment in flowing water are the velocity of flow, shear and normal stress resulting from flow turbulence (e.g., [11]). When the hydrodynamic force in a turbulent flow exceeds the resisting force of a cohesive sediment bed, the sediment is detached from the bed, and the flowing water becomes turbid. This stage is characterized by the initiation of erosion [12].

In the early 1930s, Shields [1] conducted a pioneering study on the threshold of particle movement and investigated the bed-load movement using similarity principles. Later, many researchers carried out experiments with sediments of different sizes and mineralogies and deduced the threshold velocity formula of mud by considering the cohesive forces between particles [13–22]. Smerdon and Beasley [17] conducted experiments in a flume and investigated the relationships between the shear stress of critical erosion, plasticity index, and dispersity. Partheniades [18] presented two modes of cohesive sediment erosion, i.e., surface erosion and mass erosion. In recent years, biological effect on the stabilization of sediment of mud has been studied by some researchers [23–27]. In these studies, a phenomenon known as "biostabilization" occurs, defined as "a decrease in sediment erodibility caused by biological actions" [28].

During the 1980s, Cao and Du [29] used muddy clay with different porosities to study the relationships between scour rate and shear stress on the bed. The results reported by Xu [30] show that consolidation compacting degree is the main factor influencing the critical erosion of cohesive soil. Kamphuis [31] conducted a series of studies on the erosion of cohesive soil and found that the critical shear stress of erosion is related to the plasticity index of sediment and the vane shear strength of sediment. Biological activity also affects the erosion behavior [32,33], and the erosion resistance increases with organic content [34]. Huang et al. [35] provided a model for the initiation of movement of

* Corresponding author.
E-mail address: yangb@home.swjtu.edu.cn (J. Feng).

https://doi.org/10.1016/j.apor.2018.09.006
Received 4 June 2018; Received in revised form 4 September 2018; Accepted 6 September 2018
Available online 13 September 2018
0141-1187/

cohesive soil by correlating critical shear stress and shear strength. Roberts et al. [36] evaluated the effects of particle size and bulk density on the erosion of quartz particles. They found that cohesive effects become significant as the particle size decreases. The critical shear stress depends on the bulk density and particle size.

Jin et al. [37] evaluated the effects of bentonite on the erosion rates of quartz particles. Lick et al. [38] developed a theoretical description of initiation of movement of sediments consisting of uniform-size, quartz particles. Xiao et al. [39] conducted laboratory experiments on the critical erosion of cohesive clay in a flume and discussed the effect of wet unit weight of soil on critical erosion. The results reported by Xiao et al. [39] show that the critical erosion pattern of cohesive clay is mainly suspension load. Recently, some experimental studies were conducted to determine the relationship between critical shear stress, erosion rate, and deposition rate with different mechanical, physical, electrochemical, and biological soil properties [40,41].

The mode of erosion of cohesive sediment was studied in the past. For coarse sand-clayey mud mixtures, Muray [42] found that sand moves as bed load, whereas the fines move as suspension. The visual observation of erosion processes reported by Kamphuis and Hall [31] reveals that the size of particles eroding from the bed decreases with the increase in sand content. At low shear stresses, the finer fraction is washed out, and at higher shear stresses, the larger grain size material is eroded. Amos et al. [43] reported two modes of erosion for cohesive beds: “Type 1″ erosion with a peak in the erosion rate that rapidly decreases with time, also known as “benign” erosion; “Type 2″ erosion where a high erosion rate is sustained, also known as “chronic” erosion of material from the bed.

Currently, some disagreements exist about the criterion of initiation of movement of mud. Many factors affect this problem: e.g., bulk density, particle size, size distribution, mineralogy, organic content, and size of gas bubbles) [36]. Most researchers obtained the friction velocity on the surface of mud only by measuring the mean flow velocity. In fact, for the same value of mean flow velocity, a different velocity profile corresponds to a different friction velocity. Moreover, the criterion of evaluating the initiation of movement of mud is not quantitative, and most of the existing studies determined the critical flow velocity of initiation of movement mainly by observation, leading to great subjectiveness about the results.

In this paper, a PIV velocimeter was used to measure the velocity profile to determine the friction velocity more precisely. To quantitatively determine the initiation of movement of mud, a new method is provided to determine the initiation of movement of mud by measuring the grey value of water’s image. In this study, the initiation of movement of mud with different deposition densities in unidirectional currents was investigated experimentally in a flume. A continuous current dynamo was used to drive the water pump that changes the flow in the flume.

2. Experimental details

2.1. Experimental apparatus and method

The experiment was conducted in a flume with a length of 25 m, width of 0.5 m, and height of 0.6 m. An electromagnetic flowmeter was used to measure the water flux in the flume; the mean flow velocity was obtained from the water flux. The water level was obtained from the ruler installed on the side wall of glass. A propeller-type flow meter installed at the upstream of incoming flow was also used to measure the flow velocity with an accuracy of 0.1 cm/s. A DC motor was used to drive the water pump that changes the flow flux of water in the flume, and the flow velocity is changed correspondingly.

To precisely measure the velocity profile near the bed without disturbing the flow and erosion of soil, a PIV velocimeter, a noncontact measurement method, was used. The PIV is composed of a continuous laser, Photron Fastcam SA-1.1 high-speed camera with a resolution of 1024 × 1024, and data-processing software. The frame frequency of the camera was 1000 frames per second. Therefore, the accuracy of PIV can be up to 0.001 m/s, and the space resolution is 1 mm. In the PIV measurement, the density of tracer particle with a diameter of 15 μm is 1.05 g/cm^3; the particle was used before the occurrence of erosion. When the erosion of mud occurs, another tracer particle, i.e., pollen with a diameter of 50 μm, was used to eliminate the disturbance of mud particles in the water for the measurement of flow velocity with PIV.

With the increase in flow velocity, the water gradually becomes turbid. When the erosion of mud occurs, the water becomes clearly turbid. According to the principle of image processing, an image with different turbidity has a different grey value. The grey value for pure white image is 0, and that for pure black image is 255. Therefore, water at a different flow velocity has the corresponding grey value. The sediment concentration in water is small at the initial time, and the grey value of water’s image is also small (e.g., the grey value of clear water is almost 0). When much mud is present in the water, then the sediment concentration in the water is larger, and it also has a higher grey level. During the test, the image of water at different times was recorded using a SONY camera, and the grey value of water’s image at any time can be obtained. The grey value of water’s image at the work section in the flume was regarded as the reference for each group test when the flow velocity is zero. The relative grey value of water’s image, i.e., the difference between the grey value at any time and the reference, can be also acquired. This helps to estimate the initiation of mud’s movement.

The test section was located at the middle of the flume. The cameras for PIV and grey value measurement of water’s image were placed at the side of the flume. The laser device was placed over the flume. During the initial movement of sediment, the SONY camera recorded the variation of sediment concentration in the water, providing the grey value of water’s image by image processing. The schematic of the setup is shown in Fig. 1.

The flow velocity and grey value of water’s image were measured simultaneously, and the measuring area obtained by PIV for velocity is 10 cm × 10 cm. For each velocity, the acquisition time was 5 s to 10 s, and more than 1000 frames of velocity field data were obtained using a high-speed camera during this time. Then, the time-averaged velocity was computed from those frames of velocity field data. The velocity at the position 1–2 mm distance from the surface of mud can be measured using the PIV method.

2.2. Test samples and testing procedure

The mud used in the experiments was sampled from a natural harbor (i.e., located at the Lianyungang waterway in Jiangsu Province, China), and the deposit density of in-place mud is 1.400 g/cm^3. The grain density is 2.706 g/cm^3, and the mean size of the mud (d_{50}) is 5.12 μm. This indicates that it belongs to cohesive soil. The grain size distribution curve is shown in Fig. 2.

Before each test, the mud was mixed well and evenly placed along the bottom of the flume according to the designed density of mud. The

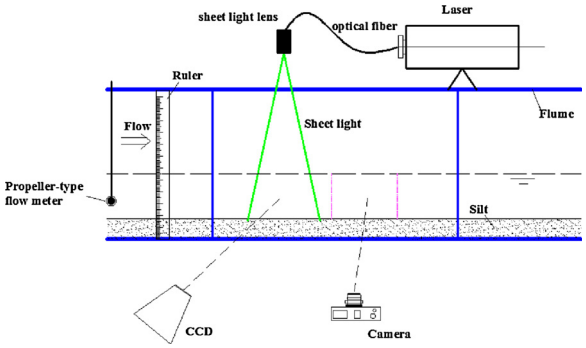

Fig. 1. Schematic of experimental setup.

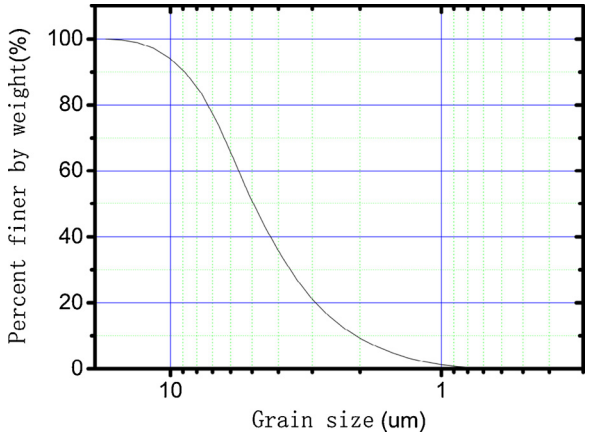

Fig. 2. Grain size distribution curve of test mud.

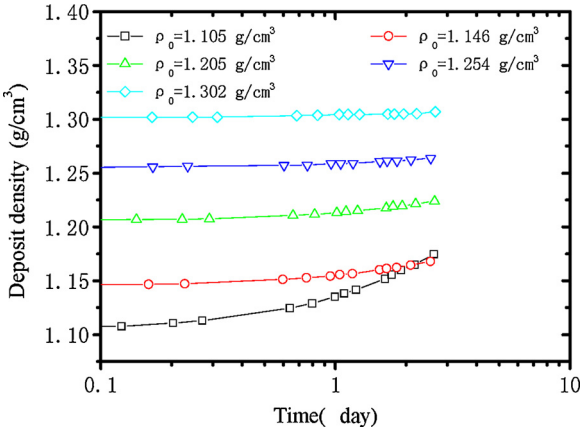

Fig. 3. Variation in deposit density with time.

thickness of mud in the test is 5 cm, and the length is 6 m. When the mud was placed in the flume, considering the soil structure, the test was conducted after the disturbed mud settled for 24 h. To investigate the variation in the density of disturbed mud sample with time, some sample mud was taken from the flume to test the deposit density. The results of the variation of deposit density with time are shown in Fig. 3. The figure shows that the deposit density slightly varies when it is larger than 1.2 g/cm^3 within 24 h. According to the trend shown in Fig. 3, the deposit density inspected in the test is well designed, and the designed deposit density of mud in the experiments is 1.155–1.400 g/cm^3. The water depth is 10 cm.

In the test, the flow velocity gradually increases from the value of 0. For each velocity from 0 to the critical flow of initiation movement of sediment at an interval, the readings of electromagnetic flow meter and propeller flow meter were recorded, and the image of water at the work section was captured using a camera to obtain the grey value of water's image. The velocity profile was also measured using PIV. Moreover, the experimental phenomenon was also visually observed to estimate the initiation of movement of mud. Six groups of tests were conducted, and the detail parameters are shown in Table 1.

3. Results and discussion

3.1. Typical characteristics of initiation of movement of mud

The experimental results show that the initiation of movement of mud can be divided into slight erosion and chunk erosion. The surface of mud is flat and smooth when the flow velocity is small (Fig. 4a). With the increase in flow velocity, local erosion occurs at the surface of mud.

Table 1
Experimental parameters for six groups of tests.

Test No.	Water depth H (cm)	Deposit density ρ_C (g/cm^3)
1	10	1.155
2	10	1.206
3	10	1.250
4	10	1.303
5	10	1.354
6	10	1.400

Some mud is lacerated from the bed, and a small sheet of mud sheds from the surface (Fig. 4b). This is defined as slight erosion. The shedding mud enters the water. At this moment, the water becomes turbid, and the flow velocity reaches up to the critical velocity corresponding to slight erosion (Fig. 4b). With the continuous increase in flow velocity, the surface of mud at several locations is heavily lacerated by the flowing water (Fig. 4c), and the water becomes more turbid (Fig. 5c). This is defined as chunk erosion.

Fig. 5 shows the image of water from the initial time to chunk erosion. The corresponding grey level image of water's image (Fig. 5) is shown in Fig. 6. Fig. 6 shows that the grey value near the surface of mud clearly varies. Therefore, a local region near the surface of mud was selected to compute the grey value of water's image, as shown in Fig. 6. The local region (rectangular block in the figure) was divided into eight parts, and the grey level value is their average value. The figure shows that the grey value of water's image significantly increases with the development of erosion. During the chunk erosion, the grey value of water's image reaches up to the maximum value.

Fig. 7 shows the variation in relative grey value of water's image with flow velocity for different deposit densities of mud. The figure shows that the relative grey value slowly varies when the flow velocity is small. The relative grey value clearly increases when slight erosion occurs, and it has a sudden increase during the chunk erosion. Fig. 7 shows that the magnitude of relative grey value has the order of 10 for slight erosion and more than 20 for chunk erosion.

To verify the correlation between sediment concentration and relative grey value of water's image, a calibration test was conducted in the laboratory. At the initial stage, a glass box with a known volume contains clear water. Then, some mud with known mass was added to the box at a time interval and mixed well every time. Because the amount of mud added to the glass box is known, the mass of mud in the water per cubic meter can be calculated each time. The image of water with a certain mud content in the glass box is photographed with camera and the corresponding to the relative grey value of image can be obtained. Finally, the relationship between sediment concentration and relative grey value was obtained, as shown in Fig. 8. Almost a linear relationship exists between the relative grey value of water and sediment concentration, as shown in Fig. 8. When the relative grey value of water has the order of ~10, the sediment concentration is about 66 g/m^3.The calibration curve also shows that the sediment concentration with a value of about 130 g/m^3 corresponds to the relative grey value of 20. According to our observation in the flume, when the sediment concentration is over 130 g/m^3, chunk erosion occurs at every place. Based on the variation in water's relative grey value with flow velocity as shown in Fig. 7 and the experimental observation of erosion, the critical flow velocity of erosion of mud was determined, as shown in Table 2. Table 2 shows two values for critical flow velocity, critical friction velocity, and critical shear stress. The upper value (smaller value) corresponds to the results of slight erosion, whereas the lower value (larger value) corresponds to those of chunk erosion. The details of relationship between critical flow velocity and critical friction velocity and shear stress are described in Section 3.2. The critical flow velocity of slight erosion for ρ_c = 1.155 g/cm^3 is 17.53 cm/s and for ρ_c = 1.400 g/cm^3 is 72.93 cm/s. The critical flow velocity of slight

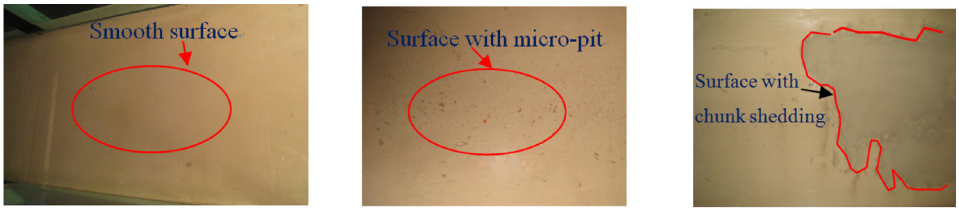

(a) initial time for no erosion(top view) (b) Slight erosion(top view) (c) chunk erosion(top view)

Fig. 4. Typical phenomenon for critical erosion of mud (ρ_c = 1.206, u = 0.366 m/s).

(a) Image of water at the initial state (u = 0) (side view) (b) Image of water for slight erosion (u = 0.252 m/s) (side view) (c) Image of water for chunk erosion (u = 0.371 m/s) (side view)

Fig. 5. Variation in the image of water with flow velocity.

erosion for ρ_c = 1.400 g/cm^3 is 4.16 times larger than that for ρ_c = 1.155 g/cm^3. This indicates that the deposit density of mud is a key factor for the initiation of movement of mud. Table 2 shows that the critical flow velocity for chunk erosion is 1.2–1.4 times larger than that for slight erosion. The critical flow velocity for chunk erosion for 1.400 g/cm^3 is up to 94.65 cm/s.

The initiation of movement of mud is mainly related to the density of particle, diameter of particle, particle-size distribution, and mineral gradient. In general, the deposit density of mud reflects the effects of the above mentioned factors. Fig. 9 shows the relationship between relative deposit density ($(\rho_c-\rho)/\rho$) and flow velocity of initiation of mud's movement (U_c). ρ is the mass density of water in the environment, and its value is 1.0105 g/cm^3. The figure shows that the deposit density of mud significantly affects the initiation of movement of mud. With the increase in deposit density of mud, the flow velocity of initiation of movement of mud also increases. Based on Fig. 9, the empirical relationship between them can be written as follows:

$$U_{c1} = 249.79\left(\frac{\rho_c - \rho}{\rho}\right) - 21.32 \quad (1)$$

$$U_{c2} = 303.19\left(\frac{\rho_c - \rho}{\rho}\right) - 20.53 \quad (2)$$

where U_{c1} is the critical flow velocity for slight erosion, and U_{c2} is the critical flow velocity for chunk erosion.

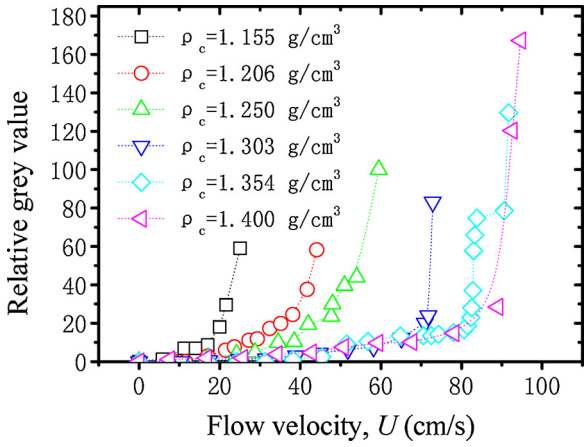

Fig. 7. Variation in water's grey value with flow velocity during critical erosion.

3.2. Friction velocity and shear stress of initiation of movement of mud

Fig. 10 shows the typical flow velocity field on the surface of mud measured by PIV. For the measurement of flow velocity, the origin of coordinate is located at the surface of mud, and the X axis is along the flow direction. Because of the good performance of PIV, the flow

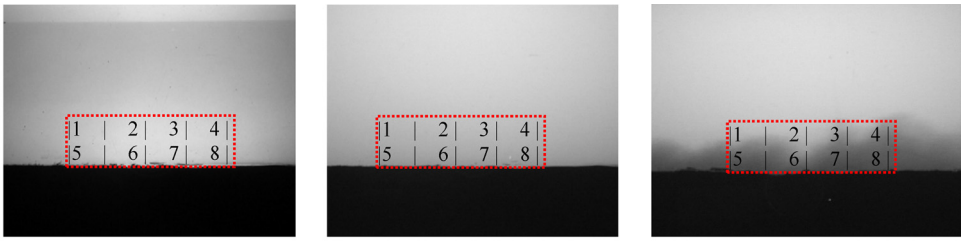

(a)Grey level image of water at initial time (u=0) (b) Grey level image of water for slight erosion (u = 0.239 m/s) (c) Grey level image of water for chunk erosion (u = 0.366 m/s)

Fig. 6. Variation in the grey level image of water with flow velocity (side view).

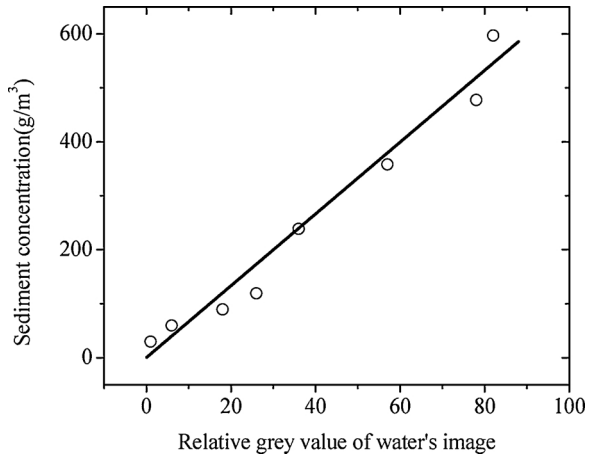

Fig. 8. Variation in sediment concentration with grey value of water's image.

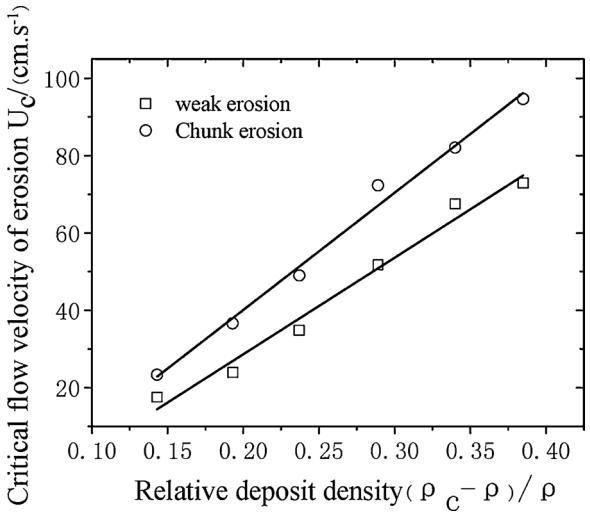

Fig. 9. Variation in critical flow velocity of erosion with relative deposit density.

velocity at the location 1–2 mm distance from the surface of mud can be measured, i.e., the flow velocity at the transition region of turbulent boundary layer can be directly measured. Notably, the color at the far left side of the image shown in Fig. 10 is the noise; therefore, the velocity at the middle of region in Fig. 10, i.e., x = 40, was used in this study. According to the velocity field measured by PIV, the flow velocity profile along the vertical direction can be obtained, and the typical profile is shown in Fig. 11. The velocity profile at logarithmic coordinate is shown in Fig. 12. The velocity profile near the wall region is clearly observed.

According to the open channel turbulence theory [44,45], the vertical time-averaged velocity distribution near the wall layer ($0 < y/H < 0.2$, H is the water depth in the open channel, y is the vertical coordinate with the origin of coordinate set at the bottom) can be expressed as follows:

$$\text{Viscous sublayer } u^+ = y^+,\ y^+ < 5 \tag{3}$$

$$\text{Turbulence logarithmic layer } u^+ = 2.5\ln y^+ + 5.5,\ y^+ > 30 \tag{4}$$

where $u^+ = \frac{\bar{u}}{u_*}$, $y^+ = \frac{u_* y}{\nu}$, $u_* = \sqrt{\frac{\tau_w}{\rho}}$, $\bar{u}$ is the time-averaged velocity, u_* is the friction velocity, ν is the kinematic viscous coefficient, τ_w is the fluid shear stress at the wall. At the turbulent zone near the wall, the relationship between time-averaged velocity $\overline{(u)}$ and the distance from the wall is a logarithmic function. According to Eq. (4), the slope rate of fitted straight line is equal to 2.5 u_*. Then, the friction velocity (u_*) can be deduced, and the shear stress on the mud bed (τ_w) is also computed. Table 2 shows the results of u_* and τ_w. The relationships between relative deposit density, critical friction velocity of erosion, and critical shear stress of erosion are shown in Figs. 13 and 14. Table 2 and Figs. 13 and 14 show that the critical friction velocity of erosion for the

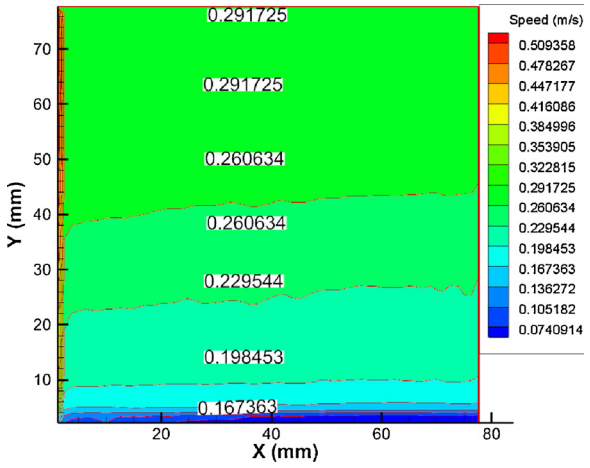

Fig. 10. Typical distribution of flow velocity field (measured by PIV).

deposit density used in this study is between 0.87 cm/s and 3.64 cm/s for slight erosion, and 1.16 cm/s and 4.73 cm/s for chunk erosion. The critical shear stress of erosion in this study is between 0.076 Pa and 1.340 Pa for slight erosion and 0.136 Pa and 2.261 Pa for chunk erosion. Both the critical friction velocity and critical shear stress of erosion increase with the increase in relative deposit density, as shown in Figs. 13 and 14.

Table 2
Test data for critical erosion of mud.

No.	Deposit density ρ_c/(g/cm^3)	Critical flow velocity for erosion U/(cm/s)	Critical friction flow velocity of erosion u_*/(cm/s)	Critical shear stress of erosion τ_c/(N/m^2)	remark
1	1.400	72.93	3.642	1.340	For slight erosion
		94.65	4.730	2.261	For chunk erosion
2	1.354	67.50	3.375	1.151	For slight erosion
		82.05	4.110	1.707	For chunk erosion
3	1.303	51.78	2.586	0.676	For slight erosion
		72.30	3.620	1.324	For chunk erosion
4	1.250	34.82	1.740	0.306	For slight erosion
		49.00	2.45	0.607	For chunk erosion
5	1.206	23.93	1.190	0.143	For slight erosion
		36.63	1.830	0.338	For chunk erosion
6	1.155	17.53	0.870	0.076	For slight erosion
		23.35	1.16	0.136	For chunk erosion

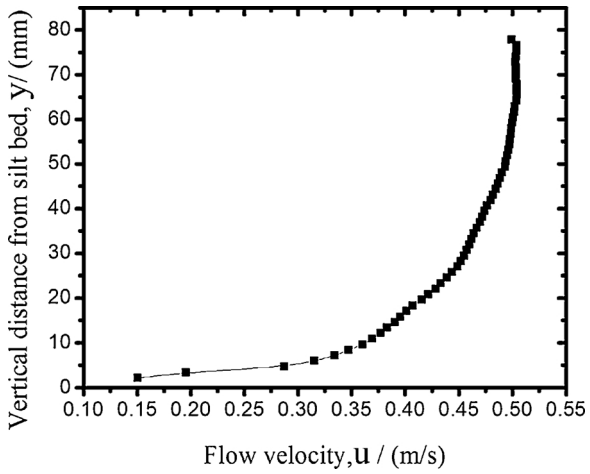

Fig. 11. Velocity profile along vertical direction (x = 40 mm).

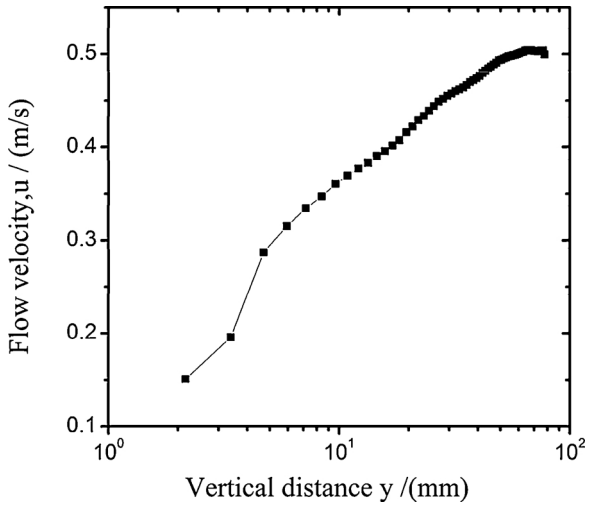

Fig. 12. Velocity profile along vertical direction at the logarithmic coordinate.

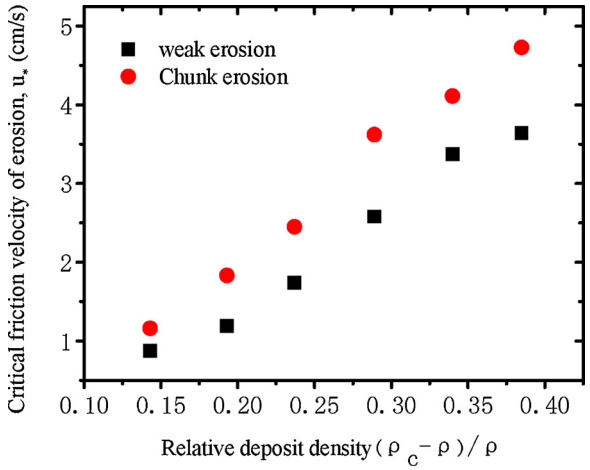

Fig. 13. Variation in critical friction velocity of erosion with relative deposit density.

4. Comparison with the previous studies

Fig. 15 shows a comparison between the present experimental results and those obtained by Hong and Ying [46], Xiao et al. [39],Yang and Wang [47], and Jiang et al. [48]. The mean grain sizes of d_{50} = 0.0066 mm and 0.0073 mm were used by Jiang et al. [48], and the mean grain size of d_{50} = 0.005 mm was used by Hong and Ying [46]. All the water depths are similar except for that reported by Xiao et al. [39]. The figure shows a relatively good consistency among the results for the case of smaller deposit density (i.e., ρ_c < 1.25 g/cm^3). However, when the value of ρ_c is larger than 1.25 g/cm^3, there are some differences between the results obtained in the present study and Jiang et al. [48]. For the case of a larger deposit density (ρ_c > 1.25 g/cm^3), the flow velocity of critical erosion reported by our study is larger than those reported by Jiang et al. [48],Yang and Wang [47], and Xiao et al. [39].

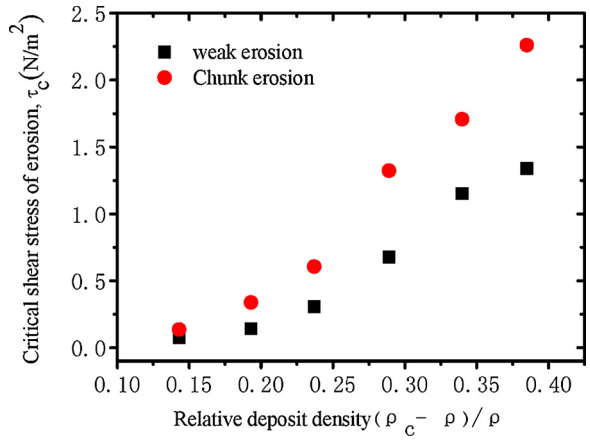

Fig. 14. Variation in critical shear stress of erosion with relative deposit density.

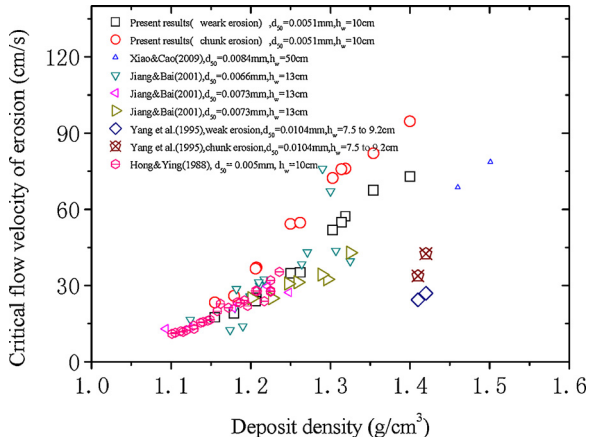

Fig. 15. Comparison with previous results.

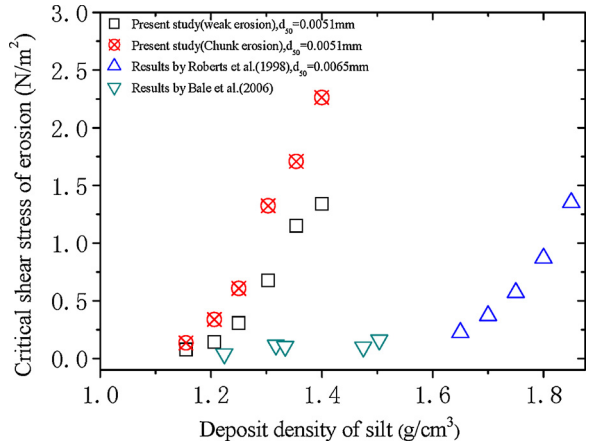

Fig. 16. Comparison with previous results.

The causes of difference between the results in the present study and those reported by Jiang et al. [48], Yang and Wang [47], and Xiao et al. [39] can be attributed to the difference of assessment criterion, consolidated statement, composition of soil, etc. The abovementioned analysis shows that complex factors affect the critical flow velocity of erosion when the deposit density is larger than 1.25 g/cm^3, and a larger diversity exists among the existing studies.

The results on the critical shear stress of erosion versus deposit density obtained in the present study, Roberts et al. [36], and Bale et al. [49] are plotted in Fig. 16. The data reported by Bale et al. [49] originates from the field measurement at the Tamar Estuary in UK. The figure shows the same trend on the variation of critical shear stress of erosion with deposit density of mud in the results reported in the present study and Roberts et al. [36], i.e., the critical shear stress of erosion increases with increasing deposit density of mud, but the magnitude of critical shear stress at the same deposit density of mud is different. The critical shear stress of erosion slightly changes with the deposit density of mud in the results reported by Bale et al. [49]. The true causes about the results reported by Bale et al. [49] were not revealed well. In our opinion, the criterion for the initiation of movement of mud is mainly qualitative, leading to a large deviation of the experimental data. The quantitative criterion to determine the initiation of movement of mud should be urgently studied. The method of relative grey value of water's image in the flume to determine the initiation movement of silt provided in this paper may contribute to this problem. A continuous study to verify this method should be conducted further.

5. Summary and concluding remarks

The initiation of movement of mixed mud sampled from a natural harbor (i.e., located at the Lianyungang waterway in Jiangsu Province, China) under the action of current was investigated experimentally. The initiation of movement of mud in unidirectional currents was determined using a new method of grey value of water's image in the flume. The flow velocity was measured using a PIV velocimeter. Some different characteristics about the initiation of movement of mud were investigated. Some conclusions are summarized as follows:

1) In this study, a new method, i.e., grey value of water's image method, to determine the initiation of movement of mud exposed to unidirectional currents is provided, and it was validated for estimating the initiation of movement of mud.
2) The initiation of movement of mud in currents can be classified as slight erosion and chunk erosion. The sediment concentration on the muddy bed is low for slight erosion, and the variation in grey value of water's image is the order of ~10 at that moment. The rate of chunk erosion corresponding to a jump in the curve of grey value of water's image clearly increases, and the variation in grey value is usually larger than the order of 20 at that moment.
3) The critical flow velocity of slight erosion for deposit density ρ_c = 1.155–1.400 g/cm^3 is in the range of 17.53–72.93 cm/s, and that of chunk erosion is in the range of 23.35–94.65 cm/s. The relationship between critical flow velocity and deposit density can be expressed as follows: $U_{c1} = 249.79(\frac{\rho_c - \rho}{\rho}) - 21.32$ and $U_{c2} = 303.19(\frac{\rho_c - \rho}{\rho} - 20.53$.
4) The critical friction velocity of erosion for the deposit density used in this study is between 0.87 cm/s and 3.64 cm/s for slight erosion, and between 1.16 cm/s and 4.73 cm/s for chunk erosion. The critical shear stress of erosion in this study is between 0.076 N/m^2 and 1.340 N/m^2 for slight erosion, and between 0.136 N/m^2 and 2.261 N/m^2 for chunk erosion. They can be calculated using the channel turbulence theory.
5) The critical flow velocity, critical friction velocity, and critical shear stress of initiation of movement of mud increase with the increase in deposit density.

Because of the complexity of this problem, many factors affect the initiation of movement of sediment. Only the deposit density of mud was considered in this study, and other factors (e.g., mineral gradient, organic gradient, cohesion of soil) should be investigated in detail. If our results will be referred in other places, the conditions may be in the range of 1.155 g/cm^3 < ρ_C < 1.400 g/cm^3, and the mean size of mud (d_{50}) is 5.12 μm. The quantitative criterion to determine the initiation of movement of mud should be urgently studied. The method of relative grey value of water's image in the flume to determine the initiation movement of silt provided in this paper may contribute to this problem. A continuous study to verify this method will be conducted further.

Acknowledgements

This work was financially supported by National Natural Science Foundation of China (Grant No.: 10902112, 51708456) and the Fundamental Research Funds for the Central Universities (2682017QY02).

References

[1] A. Shields, Anwendung der Aehnlichkeitsmechanik und der Turbulenzforschung auf die Geschiebebewegung [Application of similarity mechanics and turbulence research on shear flow] (PDF). Mitteilungen der Preußischen Versuchsanstalt für Wasserbau (in German) 26, Preußische Versuchsanstalt für Wasserbau, Berlin, 1936.
[2] M.C. Miller, I.N. McCave, P.D. Komar, Threshold of sediment motion under unidirectional currents, Sedimentology 24 (1977) 507–528.
[3] L.C. Van Rijin, Principles of Sediment Transport in Rivers, Estuaries and Coastal Seas, Aqua Publications, Zwolle, the Netherlands, 1993.
[4] R.L. Soulsby, R.J.W. Whitehouse, Threshold of sediment motion in coastal environments, Pacific Coasts & Ports Conference Vol.1 (1997) 149–154.
[5] Ning Chien, Zhaohui Wan, Mechanics of Sediment Transport, ASCE Press, 1999.
[6] A.J. Mehta, S.I. Lee, Problems in linking the threshold condition for the transport of cohesionless and cohesive sediment grain, J. Coast. Res. 10 (1994) 170–177.
[7] Bing Yang, Tao Yang, Jian-Lin Ma, Jin-Sheng Cui, The experimental study on lo-cal scour around a circular pipe undergoing vortex-induced vibration in steady flow, J. Mar. Sci. Technol. 21 (3) (2013) 250–257.
[8] A.J. Mehta, Review notes on cohesive sediment erosion, Proc. Spec. Conf. on Quantitative Approaches to Coast Sediment Access, ASCE, New York, 1988, pp. 40–53.
[9] Yang Bing, Gao Fuping, Jeng Dongsheng, Failure mode and dynamic response of a double-sided slope with high water content of soil, J. Sci. 15 (4) (2018) 859–870.
[10] E. Perret, B. Camenen, C. Berni, A. Herrero, K. El kadi Abderrezzak, Transport of moderately sorted gravel at low bed shear stresses: the role of fine sediment infiltration, Earth Surf. Process. Landf. 43 (7) (2018) 1416–1430.
[11] V.A. Vanoni, Mechanics of sediment transport and alluvial stream problems, Eng. Geol. 14 (4) (1979) 283–284.
[12] U.C. Kothyari, R.K. Jain, Influence of cohesion on incipient motion condition of sediment mixtures, Water Resour. Res. 44 (4) (2008) 368–381.
[13] Shui-chin Chang, A review on the gravitation theory of sediment suspension, Shui Li Xue Bao 3 (1963) 11–23 (in Chinese).
[14] Cunben Tang, Law of sedement's onset, Shui Li Xue Bao 2 (1963) 1–12 (in Chinese).
[15] Yuqing Sha, Dynamics of Sediment Movement, China industry press, Beijing, 1965, pp. 302–310 (in Chinese).
[16] Guoren Dou, Incipient motion of coarse and fine sediment, Shui Li Xue Bao 4 (1960) 44–60 (in Chinese).
[17] E.T. Smerdon, R.P. Beasley, Tractive Force Theory Applied to Stability of Open Channels in Cohesive Soils. Res Bull No 715, Agri Exp Sta, Univ, Missouri, 1959, pp. 60–68.
[18] E. Partheniades, Erosion and deposition of cohesive sediment, J. Hydraul. Div. ASCE 91 (1) (1965) 105–139.
[19] E. Partheniades, R.H. Cross, A. Ayora, Further results on the deposition of cohesive sediments, Proceedings of 11th Coast Enginering Conference, ASCE, New York, 1968, pp. 723–742.
[20] E. Partheniades, R.E. Paaswell, Erodibility of channels with cohesive boundary, J. Hydraul. Div. ASCE 96 (3) (1970) 755–771.
[21] C. Migniot, Etude des proprietes physiques de differer ments tres fins et de leur comportement sous des actions hydrodynamiques. La Houille Blanche, Grenoble, France, No.7, (1968), pp. 591–599 (French).
[22] W.L. Moore, F.D. Masch, Experiments on the suspension resistance of cohesive soils, J. Geophys. Res. 67 (4) (1962) 1437–1445.
[23] D.M. Paterson, R.J. Aspden, K.S. Black, Intertidal flats: Ecosystem functioning of soft sediment systems, in: G.M.E. Perillo, et al. (Ed.), Coastal Wetlands: An Integrated Ecosystem Approach, Elsevier, Netherlands, 2009, pp. 317–338.
[24] S. Fagherazzi, D. FitzGerald, R. Fulweiler, Z. Hughes, P. Wiberg, Ecogeomorphology of tidal flats, in: J.F. Shroder (Ed.), Treatise on Geomorphology, Academic Press,

San Diego, CA, 2013, pp. 201–220, , https://doi.org/10.1016/B978-0-12-374739-6.00403-6.
[25] C. Passarelli, F. Olivier, D.M. Paterson, T. Meziane, C. Hubas, Organisms as co-operative ecosystem engineers in intertidal flats, J. Sea Res. 92 (2014) 92–101, https://doi.org/10.1016/j.seares.2013.07.010.
[26] X.D. Chen, C.K. Zhang, D.M. Paterson, C.E.L. Thompson, I.H. Townend, Z. Gong, et al., Hindered erosion: the biological mediation of non-cohesive sediment behaviour, Water Resour. Res. 53 (6) (2017) 4787–4801, https://doi.org/10.1002/2016WR020105.
[27] X.D. Chen, C.K. Zhang, Z. Zhou, Z. Gong, J.J. Zhou, J.F. Tao, et al., Stabilizing effects of bacterial biofilm: EPS penetration and redistribution of bed stability down the sediment profile, J. Geophys. Res. Biogeosci. 122 (2017) 3113–3125, https://doi.org/10.1002/2017JG004050.
[28] D.M. Paterson, G.R. Daborn, Sediment stabilisation by biological action: significance for coastal engineering, in: D.H. Peregrine, J.H. Loveless (Eds.), Developments in Coastal Engineering, University of Bristol Press, Bristol, UK, 1991, pp. 111–119.
[29] Shuyou Cao, Guohan Du, Experimental study on erosion and deposition of cohesive soil, J. Sediment. Res. A Sediment. Petrol. Process. 4 (1986) 73–82 (in Chinese).
[30] Lun Xu, Experimental study on headcut scour of cohesive sedimentation in the reservoir, Institute of Water Resources and Hydropower Research Scientific Symposium. 33, Beijing: Institute of Water Resources and Hydropower Research, 1986.
[31] J.W. Kamphuis, K.R. Hall, Cohesive material erosion by unidirectional current, J. Hydraul. Div. ASCE 109 (1983) 49–61.
[32] D.M. Paterson, Short term changes in the erodibility of intertidal cohesive sediments, Liminol. Oceanogr. 34 (1989) 223–234.
[33] D.M. Paterson, R.M. Crawford, Little, Subaerial exposure and changes in the stability of intertidal estuarine sediments, Estuar. Coast. Shelf Sci. 30 (1990) 541–546.
[34] R.N. Young, J.B. Southard, Erosion of fine-grained marine sediments: sea-floor and laboratory experiments, Geol. Soc. Am. Bull. 89 (1978) 663–672.
[35] Sui-liang Huang, Zhicong Chen, Renshou Fu, Study on starting model of clay of all types, J. Hydrodyn. Ser. A 12 (1) (1997) 1–7 (in Chinese).
[36] J. Roberts, R. Jepsen, D. Gotthard, W. Lick, Effects of particle size and bulk density on erosion of quartz particles, J. Hydraul. Eng. 124 (12) (1998) 1261–1267.
[37] L. Jin, J. McNeil, W. Lick, J. Gailani, Effects of Bentonite on the Erosion Rates of Quartz Particles. Rep Prepared for the Mechanics and Environmental Engineers, Univ. of California, Santa Barbara, Calif, 2002.
[38] W. Lick, L.J. Jin, J. Gailani, Initiation of movement of quartz particles, J. Hydraul. Eng. ASCE 130 (8) (2004) 755–761.
[39] Hui Xiao, Zu-de Cao, Zaho Qun, Hong-sheng Han, Experimental study on incipient motion of coherent mud under wave and flow action, J. Sediment. Res. A Sediment. Petrol. Process. 3 (2009) 75–80 (in Chinese).
[40] X.M. Meng, Y.G. Jia, H.X. Shan, Z.N. Yang, J.W. Zheng, An experimental study on erodibility of intertidal sediments in the Yellow River delta, Int. J. Sediment Res. 27 (2012) 240–249.
[41] N. Kimiaghalam, S. Clark, H. Ahmari, An experimental study on the effects of physical, mechanical, and electrochemical properties of natural cohesive soils on critical shear stress and erosion rate, Int. J. Sediment Res. 31 (1) (2015) 1–15.
[42] W.A. Muray, Erosion of coarse sand-clayer mud mixtures, ASCE, J. Hydraul. Eng. (1977) 1222–1227.
[43] C.L. Amos, H.A. Christian, J. Grant, D.M. Paterson, A comparison of in-situ and laboratory methods to measure mudflat erodibility, in: R.A. Falconer, S.N. Chandler-Wilde, S.Q. Liu (Eds.), Hydraulic and Environmental Modelling: Coastal Waters. Proceedings of the Second International Conference on Hydraulic and Environmental Modelling of Coastal, Estuarine and River Waters 1 (1992) 325–336.
[44] G.K. Batchelor, An Introduction to Fluid Dynamics, Cambridge University Press, 1967.
[45] I. Nezu, H. Nakagawa, Turbulence in Open-Channel Flows, IAHR Monograph, A A Bakkema, 1993.
[46] Roujia Hong, Yongliang Ying, Experimental study on critical velocity of erosion of mud in currents, J. Hydraul. Eng. 8 (1988) 49–55 (in Chinese).
[47] Meiqing Yang, Guiling Wang, The incipient motion formulas for cohesive fine sediments, J. Basic Sci. Eng. 3 (1) (1995) 99–109 (in Chinese).
[48] Changbo Jiang, Yuchuan Bai, Naishen Jiang, Shixiong Hu, Incipient motion of cohesive mud in the Haihe River estuary, J. Hydraul. Eng. 6 (2001) 51–56 (in Chinese).
[49] A.J. Bale, J. Widdows, C.B. Harris, J.A. Stephens, Measurements of the critical erosion threshold of surface sediments along the Tamar Estuary using a mini-annular flume, Cont. Shelf Res. 26 (10) (2006) 1206–1216.